

## Effect of carrier emission and retrapping on luminescence time decays in InAs/GaAs quantum dots

Weidong Yang, Roger R. Lowe-Webb, Hao Lee, and Peter C. Sercel

*Department of Physics and Materials Science Institute, University of Oregon, Eugene, Oregon 97403*

(Received 14 July 1997)

We report time-resolved photoluminescence measurements as a function of temperature for InAs quantum dots grown by molecular-beam epitaxy on GaAs(100). As the temperature is increased, the decays on the high-energy side of the photoluminescence band speed up, while the decay times on the low-energy side of the band increase. This increase occurs up to a “drop” temperature, which increases with decreasing emission energy, beyond which the decay times decrease. We present a coupled rate-equation model which includes the effects of thermal emission from quantum dot states into the wetting layer followed by transport and recapture, which reproduces the dispersive temperature dependence observed. The activation energy for thermal emission from quantum dots emitting at a given frequency is found to be approximately one-half the effective band-gap difference between the quantum dot and the wetting layer. This result is consistent with detailed balance requirements under the assumption that, on average, electrons and holes are captured and emitted by quantum dots in pairs. [S0163-1829(97)07943-5]

### I. INTRODUCTION

The realization that defect-free quantum dots (QD's) may be formed directly during molecular-beam epitaxy by strain-induced islanding has spurred much experimental effort directed toward understanding and exploiting the electronic and optical properties of these structures.<sup>1-14</sup> While a general consensus has emerged on a number of important characteristics, e.g., the  $\delta$ -function-like character of the joint density of states for optical transitions,<sup>3,4</sup> there remain a number of open questions.

One major issue remaining to be addressed concerns the physics of carrier relaxation in QD's, which at present is poorly understood. An energy relaxation bottleneck has been predicted when the interlevel spacings do not match the zone-center optical-phonon energy,<sup>15-17</sup> a situation which is apparently manifested in the case of self-organized InAs quantum dots. If the bottleneck exists, it should be observable in time-resolved measurements of the photoluminescence decays. Thus far, measurements by a number of groups have failed to observe a significant bottleneck effect.<sup>12,13</sup>

Much work remains to be done in this area to identify the dominant relaxation mechanism. While many investigators have reported experimental time-resolved photoluminescence (PL) measurements on QD samples, reported analyses have so far been limited to a determination of the phenomenological luminescence decay times. In order to constrain models of carrier relaxation in QD structures, it is clear that a quantitative approach will be necessary.

With this motivation, we carried out measurements of the temperature dependence of photoluminescence time decays in self-organized InAs QD's, and developed a coupled rate-equation model to explain the observed temperature dependence. As the temperature is increased, the decays on the high-energy side of the PL band speed up. Simultaneously the decay times on the low-energy side of the band change

nonmonotonically, first increasing and then decreasing above a “drop” temperature which increases with decreasing emission energy. The slowing down effect, which has been noted before in the literature,<sup>12,13</sup> is unexpected in quantum dots. However, as described below, we have been able to account quantitatively for the temperature dependence by considering the effect of thermally activated carrier emission and retrapping. The activation energy governing thermal emission is found to be approximately equal to one-half the effective band-gap difference between quantum dots and the wetting layer. This result is consistent with detailed balance requirements under the assumption that, on average, electrons and holes are thermally emitted from QD's in pairs. While the microscopic relaxation mechanism cannot be established on the basis of this result, the phenomenology observed appears to rule out certain hypotheses which have been advanced to explain the unusual temperature dependence, such as thermal population of a dark exciton state.<sup>13</sup>

### II. SAMPLE GROWTH AND PHOTOLUMINESCENCE SPECTRA

The samples studied were grown on (100) nonintentionally-doped GaAs substrates in a custom molecular-beam-epitaxy chamber built at Oregon.<sup>5</sup> After growing a GaAs buffer layer at 590 °C the substrate temperature was lowered to 500 °C for growth of the QD's. QD growth was performed by cycled deposition of In (0.2 ML, 5 s) followed by As<sub>2</sub> (25 s, beam equivalent pressure  $5 \times 10^{-6}$  Torr). Growth was monitored by reflection high-energy electron-diffraction (RHEED) which showed a transformation to a spotty diffraction pattern indicative of island formation at a critical coverage of 1.5 ML of deposited InAs. Immediately following the final In/As cycle, the sample was capped with 30 nm of GaAs. Nonresonantly excited PL spectra of samples with InAs coverages between 1.4 and 3.0 ML are shown in Fig. 1(a). These spectra were measured with a Ge pin detector under cw excitation with the 488-nm line of

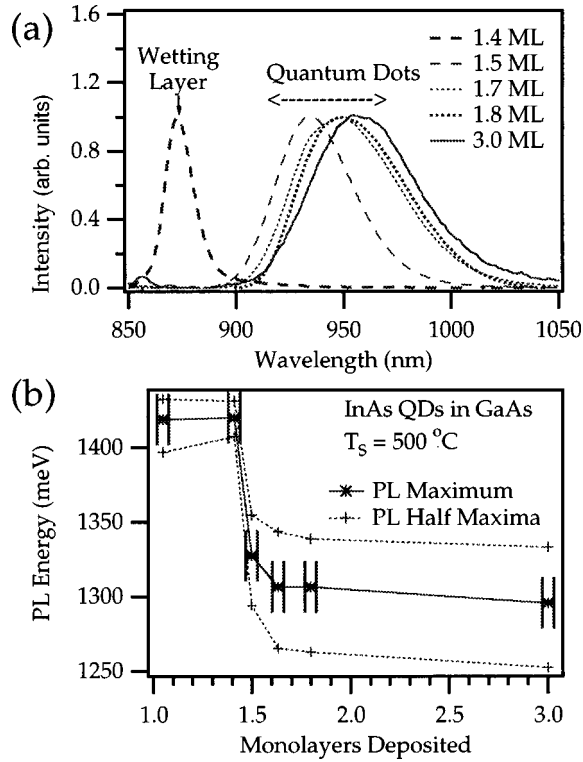


FIG. 1. Islanding transition: InAs on GaAs. (a) Photoluminescence spectra of samples with total deposited InAs between 1.4 and 3.0 ML. (b) Photoluminescence energy vs amount of InAs deposited. Both the peak energy (solid line) and the energies at half-maxima (dotted lines) are shown.

an argon-ion laser. Figure 1(b) shows the peak emission energy vs nominal InAs coverage—the sharp break at 1.5 ML coincides with the onset of the two-dimensional (2D) to 3D transition as observed during the growth by RHEED.

Note that many aspects of the electronic structure of self-organized InAs/GaAs QD's, such as the number of bound electron and hole states, remain controversial.<sup>8–11</sup> The problem of characterizing these samples is exacerbated by the fact that samples grown by different groups under nominally similar growth conditions frequently possess quite different properties.<sup>5</sup> To further characterize—and document—the properties of the samples studied in the time-resolved PL experiments discussed below, we measured PL spectra under resonant excitation. PL spectra obtained from the 1.8-ML sample, under continuous-wave excitation with a Ti sapphire laser tuned between 890 and 950 nm, are shown in Fig. 2. Luminescence was dispersed with a  $\frac{1}{4}$ -m monochromator with a 600-g/mm diffraction grating and detected with a single-photon-counting silicon avalanche photodiode (EG&G Canada SPCM). The spectra exhibit relatively sharp single LO-phonon lines at 35 and 30 meV, consistent with the strain shifted bulk InAs LO phonon and an interface mode associated with the QD's, respectively, as well as broad two- and three-phonon resonances centered at 65 and 95 meV. While similar spectra were previously reported by Heitz *et al.*,<sup>6</sup> spectra reported by others do not exhibit the single phonon line.<sup>7,9</sup> As pointed out by Steer *et al.*,<sup>9</sup> a major unresolved question concerns the origin of the “nonresonant” emission observed in addition to the multiphonon resonances discussed above. Given that the resonances re-

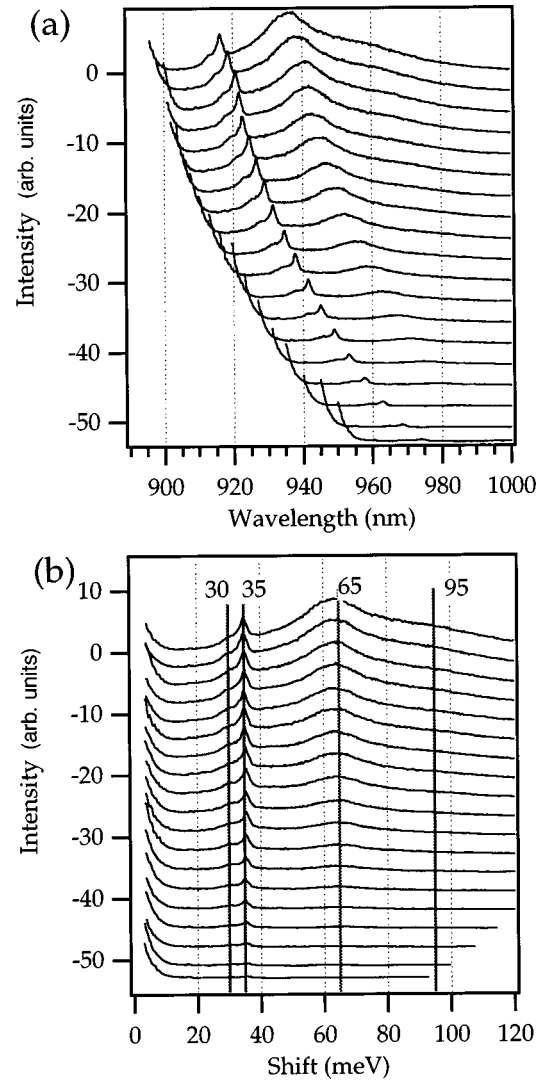


FIG. 2. Resonantly excited PL spectra of InAs/GaAs QDs with 1.8 ML of InAs. (a) PL plotted vs emission wavelength for various excitation wavelengths between 890 and 950 nm. (b) PL spectra as in (a) but plotted vs Stoke's shift from laser line. The solid vertical lines mark the energies 30, 35, 65, and 95 meV corresponding to the phonon resonances discussed in the text.

flect enhanced relaxation by emission of multiple LO phonons, by what mechanism does carrier relaxation occur in those QD's which emit at energies Stoke's shifted by amounts not equal to integer multiples of the LO-phonon energies? While a number of models have been proposed,<sup>18–22</sup> existing studies including this one do not yet permit an answer to this question.

### III. TIME-RESOLVED PHOTOLUMINESCENCE EXPERIMENTS

Time-resolved PL measurements were made over a temperature range from 10 to 140 K using a time-correlated single-photon-counting system incorporating the monochromator and silicon avalanche detector referred to in Sec. II. Samples were excited with a cavity-dumped mode-locked Ti:sapphire laser tuned to a center wavelength of 850 nm, with a 10-nm band pass set with an extracavity prism filter.<sup>23</sup>

Photoluminescence excitation studies undertaken by our group demonstrate that this pump wavelength corresponds to excitation directly into the wetting layer (WL) on which the QD's form, which has a band gap equal to 1425 meV at 10 K. We chose to pump into the wetting layer rather than the GaAs barrier to simplify the decay dynamics. Our observation has been that PL decays measured under excitation into the GaAs barrier are typically nonexponential. This is presumably due to the more spatially distributed absorption which occurs when pumping into the GaAs barrier, and the effect of surface recombination. In addition, the capture dynamics are fundamentally more complicated in the case of excitation above the GaAs band edge, because capture into QD's may in principle occur directly from the GaAs barrier or sequentially through the wetting layer.

Typical PL decays for the 1.8-ML sample are shown in Fig. 3 for temperatures of 10, 80, and 130 K, for several emission wavelengths within the PL band. Several features are apparent in these plots. First, the PL decays are well described with a single exponential over the first 4 ns of the decay, with the exception of a fast initial transient in the higher-energy decays which is probably due to excited-state emission.<sup>13,14</sup> As the temperature is increased, the decays on the high-energy side of the PL band speed up, while the decay times on the low-energy side of the band exhibit a nonmonotonic change. The decay times first increase with increasing sample temperature, and then decrease above a "drop" temperature. The drop temperature depends on the transition energy, increasing with decreasing emission energy. These features are more clearly summarized in Fig. 4, which shows the PL decay times for various emission wavelengths plotted versus sample temperature between 10 and 140 K. (The solid lines are the results of a model fit described in Sec. IV.) The luminescence decay times plotted in Fig. 4 were determined by fitting the experimental decay curves at a particular emission wavelength to a single exponential over a time window between 0.75 and 3.00 ns following the laser pulse. This delayed time window was selected to avoid the possible influence of excited-state emission on the determination of the decay times. In Fig. 4, each continuous line shows PL decay constants versus temperature for a particular emitting state at a different spectral position within the QD emission band. At  $T=10$  K, each point corresponds to emission at a distinct wavelength between 920 and 970 nm, separated by 10-nm intervals. As one moves along each line from 10 K toward higher temperatures, the wavelength at which the decay time is measured is redshifted to account for the energy-band-gap shift with temperature. The degree of shift was estimated using the energy-band-gap formula for  $\text{In}_{1-x}\text{Ga}_x\text{As}$  alloys contained in Ref. 24, with the parameter  $x$  chosen so as to match the low-temperature emission wavelength. We consider this expression for the temperature shift to be the best estimate available in the absence of detailed knowledge of the band offsets and composition of the QD's.

The slowing down effect apparent in Fig. 4 has been noted before in the literature.<sup>13</sup> However, in previous work only the decay times at the QD peak were reported, and the wavelength-dispersive character of the change in decay times with temperature, depicted in Fig. 4, was not discussed. As pointed out by several groups,<sup>12,13</sup> the increase in decay

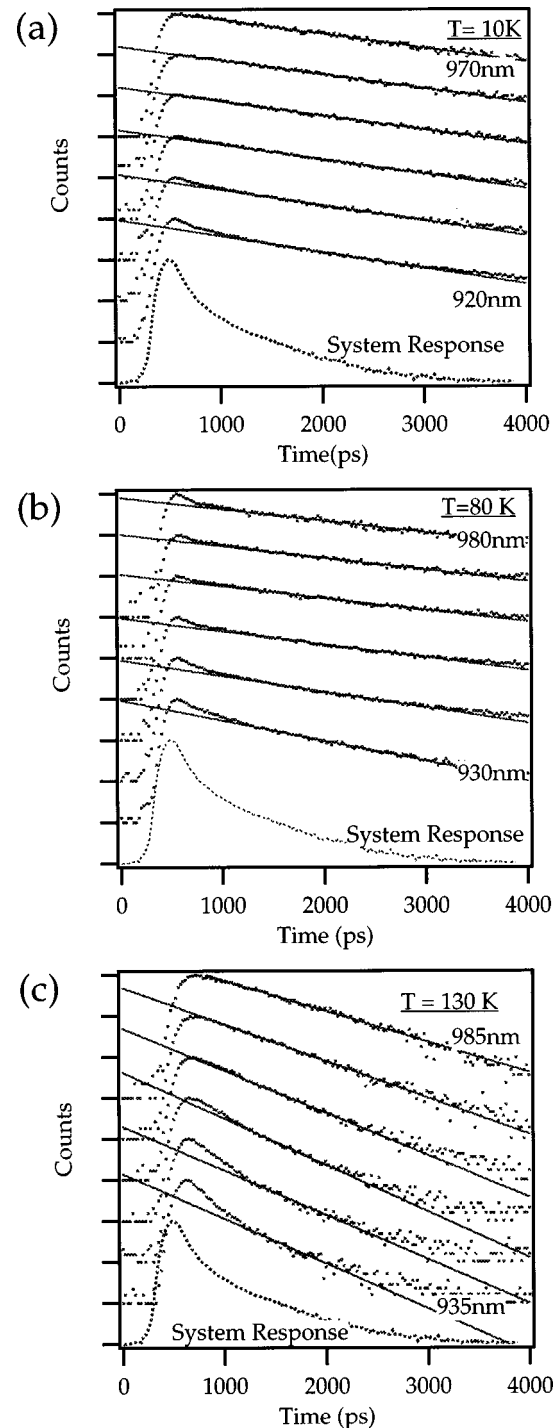


FIG. 3. Time-resolved PL spectra of InAs/GaAs QDs. The decays shown are offset vertically for clarity, and are measured at 10-nm intervals between 920 and 970 nm at  $T=10$  K (a), between 930 and 980 nm at  $T=80$  K (b), and between 935 and 985 nm at  $T=130$  K (c). The solid lines represent fits to a single exponential decay as described in the text.

times with temperature is unexpected in QD's, where the spontaneous emission rate coefficient should be independent of temperature. Note that a superficially similar increase in the lifetime of excitons in quantum wells is due to thermal population of dark exciton states away from the zone center which cannot emit, an effect which cannot occur in QD's

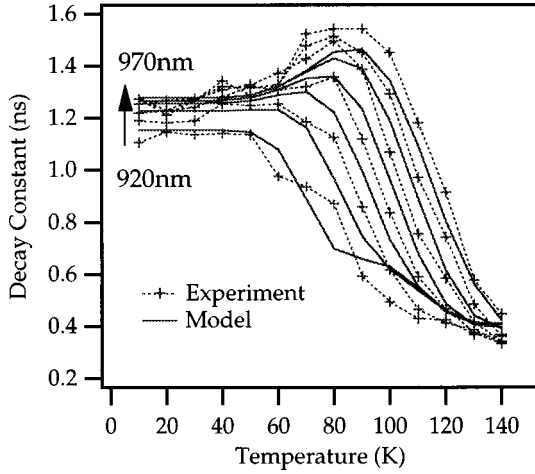


FIG. 4. PL decay times vs temperature under excitation into the WL. The crosses represent the experimental decay times, with the dotted lines providing a guide to the eye. The solid lines represent a fit to the model, Eq. (1), using the parameters listed in Table I. At  $T=10$  K, each line corresponds to an emission wavelength between 920 and 970 nm separated by 10-nm intervals. As one moves along each line from 10 K toward higher temperatures, the wavelength is redshifted to account for the energy-band-gap shift with temperature (see text).

owing to the nominally zero-dimensional character of the density of states.

The decrease in PL decay times seen at high sample temperatures, coupled with the observation that the drop temperature increases with decreasing QD emission energy, strongly suggests that the temperature dependence of the PL decays as a consequence of thermally activated emission of excitons or carriers from the QD's, followed by subsequent transport in the WL and recapture into other QD's. Specifically, we hypothesize that, at a sufficiently high temperature, QD's with higher transition energies experience a relatively large rate of thermal emission of electron-hole pairs back into the WL, leading to a reduction of the PL decay time for these QD's with increasing temperature. Meanwhile recapture from the WL causes the population of the other lower-energy QD's to be replenished during the decay, leading to an increase in the phenomenological PL decay times on the low-energy side of the PL band. At even higher temperatures, thermally activated emission ultimately begins to cause a decrease in the PL decay times of the lower-energy QD states. In Sec. IV we describe a coupled rate-equation model of the PL decay dynamics which incorporates these effects.

#### IV. RATE-EQUATION MODEL INCORPORATING THERMAL EMISSION AND RECAPTURE

To test whether or not the observed temperature dependence of the PL decay times may be understood quantitatively in terms of the hypothesis described in Sec. III, we modeled the PL time decays using a coupled rate-equation approach. The model is shown schematically in Fig. 5.

In the model, excitons are created in the WL at time  $t=0$  by absorption of a laser pulse, assumed to be a  $\delta$  function in time. The number of excitons in the WL per unit area

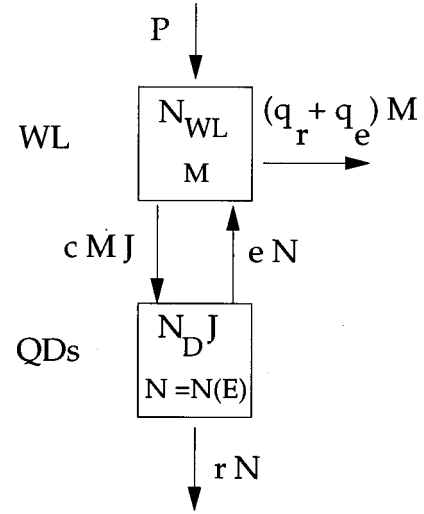


FIG. 5. Schematic of the rate-equation model described in the text.  $N_{WL}$  is the effective DOS of the WL;  $N_D$  is the areal density of QDs;  $M$  is the areal density of excitons populating the WL; and  $N=N(E)=N_D J(E)f(E)$  is the exciton population of bound QD states with energy  $E$ .  $P$  is the pump,  $c$  is the capture rate coefficient from the WL into QD bound states,  $e$  is the corresponding coefficient for emission,  $r$  and  $q_r$  are radiative recombination rate coefficients, and  $q_e$  is the rate coefficient for emission out of the WL.

at any time is  $M=N_{WL}m$ , where  $N_{WL}$  is the effective density of states of the excitons, and  $m=m(t)$  is the occupancy as a function of time  $t$ . The effective density of states is given by  $N_{WL}=D_{WL}k_B T$ , where the two-dimensional density of states in the WL is  $D_{WL}=m_{WL}/\pi\hbar^2$ . Excitons in the WL are assumed to be captured into QD's with a capture rate coefficient  $c$ , and also may be lost at a rate  $q=q_r+q_e$ . Here  $q_r$  denotes a recombination rate while  $q_e$  represents the rate of thermal emission from the WL to the GaAs barrier. The temperature dependence of this coefficient is taken to be  $q_e=q_{e0}\exp(-\Delta E/K_B T)$ , where  $\Delta E$  is the energy of the WL exciton with respect to the GaAs band edge. Once excitons are thermally emitted out of the WL, they are assumed to be irreversibly lost.

The population of QD bound excitons (or electron-hole pairs, see discussion below) at energy  $E$  with respect to the WL is given by  $N(E)=N_D J(E)f(E)$ , where the term  $N_D$  denotes the areal density of quantum dots,  $J(E)$  is a normalized density of states for bound QD excitons, and  $f(E)$  is the QD exciton occupancy. Note that  $J(E)$  reflects inhomogeneous broadening; it is taken to be a Gaussian with parameters chosen to match the peak energy and linewidth of the lowest-temperature PL spectra (10 K). The rate coefficient  $r=r(E)$  describes radiative recombination of QD bound excitons of energy  $E$ . The rate of emission from QD's back to the WL is denoted  $e$ , which is a function of the energy of the QD bound exciton, as described below in Eq. (2).

Note that we have made a significant assumption that the QD occupancy may be modeled in terms of a single distribution function  $f(E)$ . It is not clear *a priori* whether this assumption is justified. In general, capture and emission processes could involve electrons and holes independently, uncorrelated electron-hole pairs, or excitons. The first possibility is most complicated to model, since it necessitates the introduction of independent distribution functions to describe

the electron and hole occupancies, and a corresponding increase in the number of unconstrained model parameters. On the other hand, the simple model depicted in Fig. 5 would apply if one carrier type were present in excess. The model certainly applies if it is excitons or electron-hole-pairs which are captured and emitted by the QD's, in which case  $f(E)$  may be interpreted as the occupancy of QD excitons. Even if bound electron-hole pairs are uncorrelated, electrons and holes are likely captured and emitted on average in pairs since capture (emission) of one carrier type would create an electric field which would raise (lower) the emission barrier for the opposite carrier type.<sup>25</sup> Motivated by a desire for simplicity, we proceed on the assumption that it is either uncorrelated electron-hole pairs or excitons which are captured and emitted, and will judge the appropriateness of the assumption by a comparison of the model to the experimental results depicted in Figs. 3 and 4.

The populations  $M=M(t)$  and  $N=N(E;t)$  are determined by the following rate equations, which correspond to the model depicted in Fig. 5:

$$\frac{dM}{dt} = -(q_r + q_e + c)M + \int dE N e, \quad (1)$$

$$\frac{dN}{dt} = cMJ - (r + e)N.$$

These coupled equations are solved subject to the initial condition that at time zero the wetting layer has a population  $P$  ( $P \ll N_{\text{WL}}$ ) representing the number of excitons generated per unit area by absorption of the pump pulse.

In these equations the emission and capture rate coefficients are related by the detailed balance requirement in terms of the thermal equilibrium populations  $M_{\text{eq}}$  and  $N_{\text{eq}}$ .

$$cM_{\text{eq}}J = eN_{\text{eq}},$$

$$\frac{e}{c} = \frac{N_{\text{WL}}}{N_D} \beta(E),$$

$$\beta(E) = \frac{m_{\text{eq}}}{f_{\text{eq}}} \equiv \exp(-E/\nu k_B T). \quad (2)$$

In the latter equation the term  $\beta(E) \equiv \exp(-E/\nu k_B T)$  appears in the terms describing thermally activated emission from QD bound states back into the WL according to the requirement of detailed balance. Note that we have inserted a fitting parameter  $\nu$  in the expression for  $\beta$ . The value assumed by this parameter will reflect the nature of the capture and emission process. For example, the value  $\nu=1$  corresponds to equating the thermal activation energy for emission to the difference in transition energies between the emitting QD state and the lowest exciton state of the WL, as would be appropriate in the case of exciton capture and emission. As described in detail below, a value  $\nu > 2$  would be

TABLE I. Parameters used to calculate PL decays.

Constrained parameters	Value
$N_D$	$10^{10} \text{ cm}^{-2}$
$m_{\text{WL}}$	$0.40m_0$
$1/r$	1.15–1.28 ns (see Fig. 4)
Fit parameters	Value
$c$	$8.5 \times 10^9 \text{ s}^{-1}$
$q_r$	$6.5 \times 10^9 \text{ s}^{-1}$
$q_{e0}$	$5 \times 10^{12} \text{ s}^{-1}$
$\nu$	2

expected if single-carrier emission dominates, while if electrons and holes are emitted on average in pairs we expect a value  $\nu \approx 2$ .

The time-dependent distribution function  $f(E;t)$  is determined for a given temperature by solving Eq. (1). The calculated PL time decays for each energy are then convolved with the system response function, and fitted to single exponentials over the time window 0.75–3.0 ns to arrive at effective decay constants  $\tau(E)$  for each temperature. In practice, the model parameters  $c$ ,  $\nu$ ,  $q_{e0}$ , and  $q_r$  are chosen to minimize the variance between the model decay constants and the experimentally determined decay times for each energy as a function of temperature. The optimization is performed by simultaneous nonlinear least-squares fitting. Other parameters are constrained by independent measurement or by assumption. The QD density  $N_D \approx 10^{10} \text{ cm}^{-2}$  is estimated from TEM micrographs of similar samples, and the density of states in the WL is calculated assuming an exciton effective mass of  $0.4m_0$ . The radiative transition rate coefficient  $r(E)$  is assumed to be temperature independent, and is constrained to reproduce the experimental low-temperature PL lifetimes. An optimized fit to the experimental time decays, using the parameter values summarized in Table I, is presented in Fig. 4 (solid lines).

Despite its simplicity, the model reproduces the temperature dependence of the PL decay times plotted in Fig. 4. The values found for the parameters  $c$ ,  $q_{e0}$ , and  $q_r$ , listed in Table I, are physically reasonable. Surprisingly the activation energy governing thermal emission from quantum dots emitting at a given energy is found to be approximately equal to one-half the effective band-gap difference between the quantum dot and the wetting layer, corresponding to the parameter  $\nu \approx 2$ . We expected a value  $\nu = 1$ ; however, attempts to fit the time decays by constraining the parameter  $\nu$  to a value of unity were completely unsuccessful. The value  $\nu \approx 2$  is approximate since an increase (decrease) in the value of parameter  $\nu$  above (below) 2 may be effectively offset to some degree by a decrease (increase) in the values of the parameters  $c$  and  $q$ . We have found that acceptable fits with physically reasonable values for these parameters may be obtained over the range ( $1.8 < \nu < 2.2$ ).

As a check of this result we also compared the measured time-integrated PL yield versus temperature to the prediction of the model represented by Eq. (1). The time integrated PL yield is plotted in Arrhenius form in Fig. 6, along with the model result calculated using the same parameters listed in

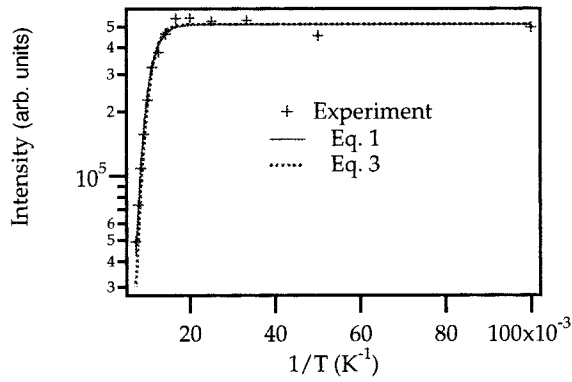


FIG. 6. Integrated PL yield vs temperature. The solid line is a calculated with Eq. (1), while the dashed line is calculated using the simplified model represented by Eq. (3). In both cases the parameters used are listed in Table I.

Table I. To clarify the effect of the parameter  $\nu$  further, we also calculated the time-integrated PL with a simple analytical expression, which is easily derived from Eq. (1) under the assumption that the PL line shape is a  $\delta$  function centered at the QD emission peak  $\bar{E}$ :

$$\int_0^{\infty} f(\bar{E}; t) dt = \frac{P}{1 + \frac{q}{c} + \frac{q}{r} \frac{N_{WL}}{N_D} \beta(\bar{E})}. \quad (3)$$

Here parameter  $P$  is a simple scaling factor, and the other parameters have the meanings defined above. The best fit again corresponds to a parameter value  $\nu \approx 2$ . The dashed line plot depicted in Fig. 6 was calculated with Eq. (3) using the parameters listed in Table I, which the reader will recall were determined by fitting the temperature dependence of the PL time decay constants. This simplified model shows that the value of parameter  $\nu$  is greatly constrained by the slope of an Arrhenius plot of the logarithm of the PL yield versus inverse temperature.

Our interpretation of the parameter value  $\nu \approx 2$  is that electrons and holes are thermally emitted from quantum dots on average in *pairs* rather than separately, a result which may be understood on the basis of detailed balance requirements.<sup>25</sup> The argument is based upon the observation that when electrons and holes are created in pairs, as in an intrinsic semiconductor, the thermal equilibrium densities of electrons and holes,  $n_{eq}$  and  $p_{eq}$ , respectively, are given by the well-known expression

$$n_{eq} = p_{eq} = \sqrt{N_c N_v} \exp(-E_g/2k_b T). \quad (4)$$

Using this result in Eq. (2) yields the result  $\nu = 2$ . That electrons and holes are likely captured and emitted on average in pairs is not surprising since capture (emission) of one carrier type would create an electric field which would raise (lower) the emission barrier for the opposite carrier type.<sup>25</sup> The same behavior with  $\nu \approx 2$  has been observed for thermal emission

of excitons from quantum wells,<sup>25</sup> although other groups performing similar experiments on quantum wells have obtained the result  $\nu = 1$ .<sup>26-28</sup> The reason for the discrepancy was ascribed in Refs. 25 and 27 to a difference in the injection level between the two sets of experiments, but the arguments presented in these papers are incomplete and mutually inconsistent. However, it is clear that exciton emission and capture would necessarily require  $\nu = 1$  on the basis of the detailed balance requirement. We speculate that the value  $\nu \approx 2$  found here is related to the fact that the QDs studied exemplify the strong confinement regime, where Coulomb-induced electron-hole correlations should be weak.<sup>29</sup>

An alternative interpretation of a parameter value  $\nu > 1$  is that the temperature dependence of the PL decay constants is due to single-carrier emission rather than pair emission, as we assumed in deriving Eq. (1). If this interpretation were correct the parameter  $\nu$  should in fact be larger than 2, since the more weakly bound carrier type would determine the activation energy for emission. In this case a value  $\nu \approx 2$ , as we found in our analysis of the experimental data, seems improbable in light of theoretical expectations that the hole binding energy should be significantly smaller than the electron binding energy in this system.<sup>10,11</sup>

A third possibility is that the temperature dependence is due to thermal population of bound QD *excited* states, which would tend to slow the PL decays at higher temperatures.<sup>13</sup> We consider this model to be incorrect since it predicts a dispersive character opposite to that which we observe. Specifically, smaller QDs should have larger excited-state splittings than larger QDs, therefore the PL decays on the higher-energy side of the PL band should begin to slow down at higher temperatures than on the low-energy side. This expectation is in direct conflict with the data presented in Figs. 3 and 4.

## V. CONCLUSIONS

We have presented measurements of the temperature dependence of photoluminescence time decays in quantum dots, which are explained quantitatively in terms of a coupled rate-equation model which includes the effects of electron-hole-pair emission and retrapping. The activation energy governing thermal emission is found to be approximately one-half the effective band-gap difference between quantum dots and the wetting layer. While the microscopic carrier relaxation mechanism cannot be established on the basis of this result, the phenomenology observed appears to rule out certain hypotheses which have been advanced to explain the unusual temperature dependence, such as thermal population of a dark exciton state. Investigation of the effects of pump fluence, background doping level, etc., should further clarify the phenomenology, and may ultimately lead to an understanding of the microscopic carrier relaxation mechanisms important in InAs QDs.

## ACKNOWLEDGMENTS

This material was based upon work supported by the National Science Foundation under Grant No. DMR 9304537, and the Army Research Office under Grant Nos. DAAH 04-95-1-0379 and DAAH04-96-1-0091.

- <sup>1</sup>L. Goldstein, F. Glas, J. Y. Marzin, M. N. Charasse, and G. LeRoux, *Appl. Phys. Lett.* **47**, 1099 (1985).
- <sup>2</sup>D. Leonard, M. Krishnamurthy, C. M. Reaves, S. P. Denbaars, and P. M. Petroff, *Appl. Phys. Lett.* **63**, 3203 (1993).
- <sup>3</sup>J.-Y. Marzin, J.-M. Gerard, A. Izrael, D. Barrier, and G. Bastard, *Phys. Rev. Lett.* **73**, 716 (1994).
- <sup>4</sup>M. Grundmann, J. Christen, N. N. Ledentsov, J. Bohrer, D. Bimberg, S. S. Ruvimov, P. Werner, U. Richter, U. Gosele, J. Heydenreich, V. M. Ustinov, A. Yu. Egorov, A. E. Zhukov, P. S. Kop'ev, and Zh. I. Alferov, *Phys. Rev. Lett.* **74**, 4043 (1995).
- <sup>5</sup>Hao Lee, Weidong Yang, and Peter C. Sercel, *Phys. Rev. B* **55**, 9757 (1997).
- <sup>6</sup>R. Heitz, M. Grundmann, N. N. Ledentsov, L. Eckey, M. Veit, D. Bimberg, V. M. Ustinov, A. Yu. Egorov, A. E. Zhukov, P. S. Kop'ev, and Zh. I. Alferov, *Appl. Phys. Lett.* **68**, 361 (1996).
- <sup>7</sup>S. Fafard, J. L. Merz, and P. M. Petroff, *Appl. Phys. Lett.* **65**, 1388 (1994).
- <sup>8</sup>K. H. Schmidt, G. Medeiros-Ribeiro, M. Oestreich, P. M. Petroff, and G. H. Dohler, *Phys. Rev. B* **54**, 11 346 (1996).
- <sup>9</sup>M. J. Steer, D. J. Mowbray, W. R. Tribe, M. S. Skolnick, M. D. Sturge, M. Hopkinson, A. G. Cullis, C. R. Whitehouse, and R. Murray, *Phys. Rev. B* **54**, 17 738 (1996).
- <sup>10</sup>M. Grundmann, N. N. Ledentsov, O. Stier, D. Bimberg, V. M. Ustinov, P. S. Kop'ev, and Zh. I. Alferov, *Appl. Phys. Lett.* **68**, 979 (1996).
- <sup>11</sup>J.-Y. Marzin and G. Bastard, *Solid State Commun.* **92**, 437 (1994).
- <sup>12</sup>G. Wang, S. Fafard, D. Leonard, J. E. Bowers, J. L. Merz, and P. M. Petroff, *Appl. Phys. Lett.* **64**, 2815 (1994).
- <sup>13</sup>Haiping Yu, Sam Lycett, Christine Roberts, and Ray Murray, *Appl. Phys. Lett.* **69**, 4087 (1996).
- <sup>14</sup>S. Raymond, S. Fafard, P. J. Poole, A. Wojs, P. Hawrylak, S. Charbonneau, D. Leonard, R. Leon, P. M. Petroff, and J. L. Merz, *Phys. Rev. B* **54**, 11 548 (1996).
- <sup>15</sup>U. Bockelmann and G. Bastard, *Phys. Rev. B* **42**, 8947 (1990).
- <sup>16</sup>H. Benisty, C. M. Sotomayor-Torres, and C. Weisbuch, *Phys. Rev. B* **44**, 10 945 (1991).
- <sup>17</sup>H. Benisty, *Phys. Rev. B* **51**, 13 281 (1995).
- <sup>18</sup>T. Inoshita and H. Sakaki, *Phys. Rev. B* **46**, 7260 (1992).
- <sup>19</sup>U. Bockelmann and T. Egeler, *Phys. Rev. B* **46**, 15 574 (1992).
- <sup>20</sup>Al. L. Efros, V. A. Kharchenko, and M. Rosen, *Solid State Commun.* **93**, 281 (1995).
- <sup>21</sup>Peter C. Sercel, *Phys. Rev. B* **51**, 14 532 (1995).
- <sup>22</sup>Darrell F. Schroeter, David J. Griffiths, and Peter C. Sercel, *Phys. Rev. B* **54**, 1486 (1996).
- <sup>23</sup>D. S. Alavi, M. G. Raymer, and P. C. Sercel (unpublished).
- <sup>24</sup>S. Adachi, *Physical Properties of III-V Semiconductor Compounds* (Wiley, New York, 1992), p. 104.
- <sup>25</sup>P. Michler, A. Hangleiter, M. Moser, M. Geiger, and F. Scholz, *Phys. Rev. B* **46**, 72 880 (1992).
- <sup>26</sup>G. Bacher, H. Schweizer, J. Kovac, A. Forchel, N. Nickel, W. Schlapp, and R. Losch, *Phys. Rev. B* **43**, 9312 (1991).
- <sup>27</sup>G. Bacher, C. Hartmann, H. Schweizer, T. Held, G. Mahler, and N. Nickel, *Phys. Rev. B* **47**, 9545 (1993).
- <sup>28</sup>M. Vening, D. J. Dunstan, and K. P. Homewood, *Phys. Rev. B* **48**, 2412 (1993).
- <sup>29</sup>Garnett W. Bryant, *Phys. Rev. B* **37**, 87 633 (1988).